ensure sufficient expression of the encoded protein in the focus formation assay. We have therefore now constructed a retroviral cDNA expression library from a human PDC cell line, MiaPaCa-2, and tested this library in the focus formation assay with 3T3 cells. For library construction, we took advantage of a polymerase chain reaction (PCR) system that preferentially amplifies full-length cDNAs. The resulting library had sufficient complexity with a high percentage of full-length cDNAs. With this library, we have revealed that the lymphotoxin-β receptor (LTBR) gene possesses transforming activity.

Materials and methods

Cell lines and culture. MiaPaCa-2, NIH 3T3, and BOSC23 cell lines were obtained from American Type Culture Collection and maintained in Dulbecco's modified Eagle's medium (DMEM)–F12 (Invitrogen, Carlsbad, CA) supplemented with 10% fetal bovine serum (Invitrogen) and 2 mM L-glutamine.

Construction of retroviral cDNA expression library. Total RNA extracted from MiaPaCa-2 cells with the use of an RNeasy Mini column and RNase-free DNase (Qiagen, Valencia, CA) was subjected to first-strand cDNA synthesis with PowerScript reverse transcriptase, SMART IIA oligonucleotide, and CDS primer IIA (Clontech, Palo Alto, CA). The resulting cDNAs were amplified for 14 cycles with 5′ PCR primer IIA and a SMART PCR cDNA synthesis kit (Clontech), with the exception that LA *Taq* polymerase (Takara Bio, Shiga, Japan) was substituted for the Advantage 2 DNA polymerase provided with the kit. The amplified cDNAs were treated with proteinase K, rendered blunt-ended with T4 DNA polymerase, and ligated to the BstXI-adaptor (Invitrogen). Unbound adaptors were removed with the use of a cDNA size-fractionation column (Invitrogen), and the remaining cDNAs were ligated into the BstXI site of the pMXS retroviral plasmid (kindly provided by T. Kitamura, Institute of Medical Science, University of Tokyo). The resulting pMXS-cDNA plasmids were introduced into ElecroMax DH10B cells (Invitrogen) by electroporation.

Focus formation assay. BOSC23 cells (1.8×10^6) were seeded into a 6-cm culture dish, cultured for 24 h, and then transfected with 2 μg of retroviral plasmids mixed with 0.5 μg of pGP plasmid (Takara Bio), 0.5 μg of pE-eco plasmid (Takara Bio), and 18 μl of Lipofectamine reagent (Invitrogen). Two days after transfection, polybrene (Sigma, St. Louis, MO) was added to the culture supernatant at a concentration of 4 μg/ml, and the supernatant was subsequently used to infect 3T3 cells for 48 h. The culture medium of the 3T3 cells was then changed to DMEM-F12 supplemented with 5% calf serum and 2 mM L-glutamine, and the cells were cultured for 2 weeks.

Recovery of cDNAs from transformants. Transformed 3T3 cell clones were harvested with a cloning syringe and cultured independently in 10-cm culture dishes. Genomic DNA was extracted from each clone by standard procedures and then subjected to PCR with 5′ PCR primer IIA and LA *Taq* polymerase for 50 cycles of 98 °C for 20 s and 68 °C for 6 min. Amplified DNA fragments were purified by gel electrophoresis and ligated into the pT7Blue-2 vector (EMD Biosciences, San Diego, CA) for nucleotide sequencing.

Anchorage-independent growth in soft agar. 3T3 cells (2×10^6) were infected with a retrovirus encoding a truncated form of LTBR or activated KRAS2 (see Results), resuspended in the culture medium supplemented with 0.4% agar [SeaPlaque GTG agarose (Cambrex, East Rutherford, NJ)], and seeded onto a base layer of complete medium supplemented with 0.5% agar. Cell growth was assessed after culture for 2 weeks.

Tumorigenicity assay in nude mice. 3T3 cells (2×10^6) infected with a retrovirus either encoding the truncated form of LTBR or containing the human wild-type LTBR cDNA (GeneCopoeia, Germantown, MD) were resuspended in 500 μl of phosphate-buffered saline and injected into each shoulder of a nu/nu Balb-c mouse (6-weeks old). Tumor formation was assessed after 3 weeks.

5′-Rapid amplification of cDNA ends (RACE). 5′-RACE was performed as described [8]. In brief, total RNA extracted from MiaPaCa-2 cells was used to generate cDNAs with an LTBR-specific primer (5′-GCAGTGGCTGTACCAAGTCA-3′). Excess primer was removed with a microconcentrator (Amicon, Austin, TX), and a poly(A) tail was added to the cDNAs by incubation with dATP and terminal deoxynucleotidyltransferase (Invitrogen). The first PCR was performed with the dT-adaptor primer (5′-GACTCGAGTCGACATCGATTTTTTTTTTTTT TTTT-3′) and RACE-1 antisense primer (5′-CTCCCAGCTTCCAGCT ACAG-3′), and the second PCR with the adaptor primer (5′-GACTCGA GTCGACATCG-3) and RACE-2 antisense primer (5′-GAGCAGAAA GAAGGCCAGTG-3′). The amplification protocol for the first PCR comprised incubation at 94 °C for 2 min followed by 20 cycles of 94 °C for 1 min, 55 °C for 1 min, and 72 °C for 3 min. That for the second PCR included incubation at 94 °C for 2 min followed by 30 cycles of 94 °C for 1 min, 53 °C for 1 min, and 72 °C for 3 min.The final PCR products were ligated into pT7Blue-2 for nucleotide sequencing.

Results

Screening for transforming genes by focus formation assay

To screen for transforming genes in PDC, we constructed a cDNA expression library from MiaPaCa-2 cells. Full-length cDNAs were selectively amplified by a PCR protocol from total RNA isolated from the cells and were ligated into the retroviral vector pMXS. We obtained a total of 1.2×10^6 colony-forming units of independent library clones, from which we randomly selected 30 clones and examined the incorporated cDNAs. An insert of $\geqslant 500$ bp was present in 24 (80%) of the 30 clones and the average size of these 24 inserts was 1.84 kbp.

Introduction of the library plasmids into a packaging cell line yielded a recombinant retroviral library that was used to infect mouse NIH 3T3 fibroblasts. After culture of the infected cells for 2 weeks, a total of 18 transformed foci were identified. No foci were observed for 3T3 cells infected with the empty virus. Each transformed focus was isolated, expanded, and used to prepare genomic DNA. PCR amplification of the inserts identified a total of 29 cDNA fragments, each of which was ligated into a cloning vector and subjected to nucleotide sequencing from both ends. Screening of the 29 cDNA sequences against the public nucleotide sequence databases revealed that they showed >95% sequence identity to 13 independent genes, 11 known and 2 unknown (Table 1).

To confirm the transforming ability of the isolated cDNAs, we again ligated them into pMXS and used the corresponding retroviral vectors to re-infect 3T3 cells. Two of the 13 independent genes (clone ID #4, corresponding to *LTBR* [GenBank Accession No. NM_002342]; clone ID #10, corresponding to *KRAS2* [GenBank Accession No. NM_004985]) reproducibly induced the formation of transformed foci in 3T3 cells (Fig. 1). Further sequencing our *KRAS2* cDNA revealed that it has a point mutation leading to the amino acid change from a glycine residue at position 12 to a cysteine (data not shown). Whereas the oncogenic potential of mutated *KRAS2* has been

Table 1
MiaPaCa-2 cell cDNAs isolated from 3T3 transformants

Clone ID #	Gene symbol	GenBank No.	Presence of entire ORF
1	CGI-152	NM_020410	Yes
2	RAB28	NM_004249	Yes
3	MRPL43	NM_032112	Yes
4	LTBR	NM_002342	No
5	UBQLN1	NM_013438	Yes
6	TBC1D2	NM_018421	Yes
7	FKBP10	NM_021939	Yes
8	HCCA2	NM_053005	Yes
9	Unknown	AK123415	ND
10	KRAS2	NM_004985	Yes
11	STK11IP	NM_052902	Yes
12	Unknown	AA627562	ND
13	PFKP	NM_002627	Yes

ORF, open reading frame; ND, not determined.

extensively investigated [3], little is known of such activity for *LTBR*. We thus focused on *LTBR* for further analysis.

Identification of a truncated form of LTBR

Although the nucleotide sequence of both ends of our LTBR cDNA was identical to that of human *LTBR*, the size of our cDNA (1452 bp) was smaller than that (2136 bp) of the full-length cDNA previously described. We thus determined the complete nucleotide sequence of our cDNA, revealing that it starts at nucleotide position 685 of the reported sequence (NM_002342). The longest open reading frame in our cDNA begins at amino acid position 221 and ends at position 435 of the previously described LTBR protein; it therefore encodes a predicted protein of 215 amino acids with a calculated molecular mass of 22,692 Da (Fig. 2). Given that the nucleotide sequence surrounding the putative translation start site of our cDNA matches the consensus Kozak motif, the corresponding mRNA likely produces this NH_2-terminally truncated form of LTBR, which is hereafter referred to as short-type LTBR.

5′-RACE analysis of LTBR mRNA

To confirm the presence of an mRNA encoding short-type LTBR in MiaPaCa-2 cells, we performed 5′-RACE to determine the 5′ ends of LTBR mRNAs. The first strand of LTBR cDNAs was generated with an LTBR-specific reverse transcription (RT) primer (Fig. 2) from RNA isolated from MiaPaCa-2 cells. Poly(A) was added to the 3′ end of the cDNAs, which were then subjected to nested PCR in order to amplify the 5′ ends. PCR products (ranging from a few hundred to 2000 bp) were detected only when reverse transcriptase was included in the procedure (Fig. 3A), indicating that the products were synthesized from cDNA, not from genomic DNA. The nucleotide sequence of 96 randomly chosen PCR products was determined. Sixty-eight of the 96 products matched the LTBR cDNA sequence and the positions of their 5′ ends are indicated in Fig. 3B. Transcription of most of the mRNAs corresponding to these PCR products was initiated in the region immediately upstream of the translation start site for short-type LTBR, indicating the existence of multiple mRNAs for this truncated protein in vivo.

Confirmation of transforming activity of short-type LTBR

To confirm the transforming activity of short-type LTBR, we examined its effect on anchorage-independent growth of 3T3 cells in soft agar. Whereas cells infected with an empty virus did not grow in soft agar, those infected with a virus encoding short-type LTBR formed multiple foci in repeated experiments (Fig. 4A). In addition, 3T3 cells expressing activated *KRAS2* readily grew in the agar.

We also injected the infected cells into nude mice. Tumors formed at all ($n = 10$) sites injected with 3T3 cells expressing short-type LTBR (Fig. 4B). Again, 3T3 cells expressing activated *KRAS2* also generated tumors at a high frequency, whereas those infected with the empty virus did not induce tumor formation. Together, these results thus confirmed that short-type LTBR possesses transforming activity.

Transforming activity of wild-type LTBR

To determine whether the full-length (435-amino acid) LTBR protein also possesses oncogenic potential, we performed the focus formation assay and in vivo tumorigenicity assay with a recombinant retrovirus encoding the wild-type

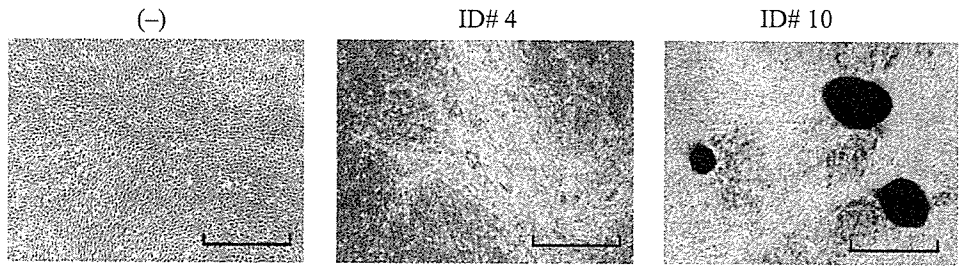

Fig. 1. Identification of transforming genes of MiaPaCa-2 cells. Mouse 3T3 cells were infected with an empty retrovirus (–) or with recombinant retroviruses harboring cDNAs corresponding to library clones ID #4 (short-type LTBR) or ID #10 (KRAS2). The cells were photographed after culture for 2 weeks. Scale bars, 1 mm.

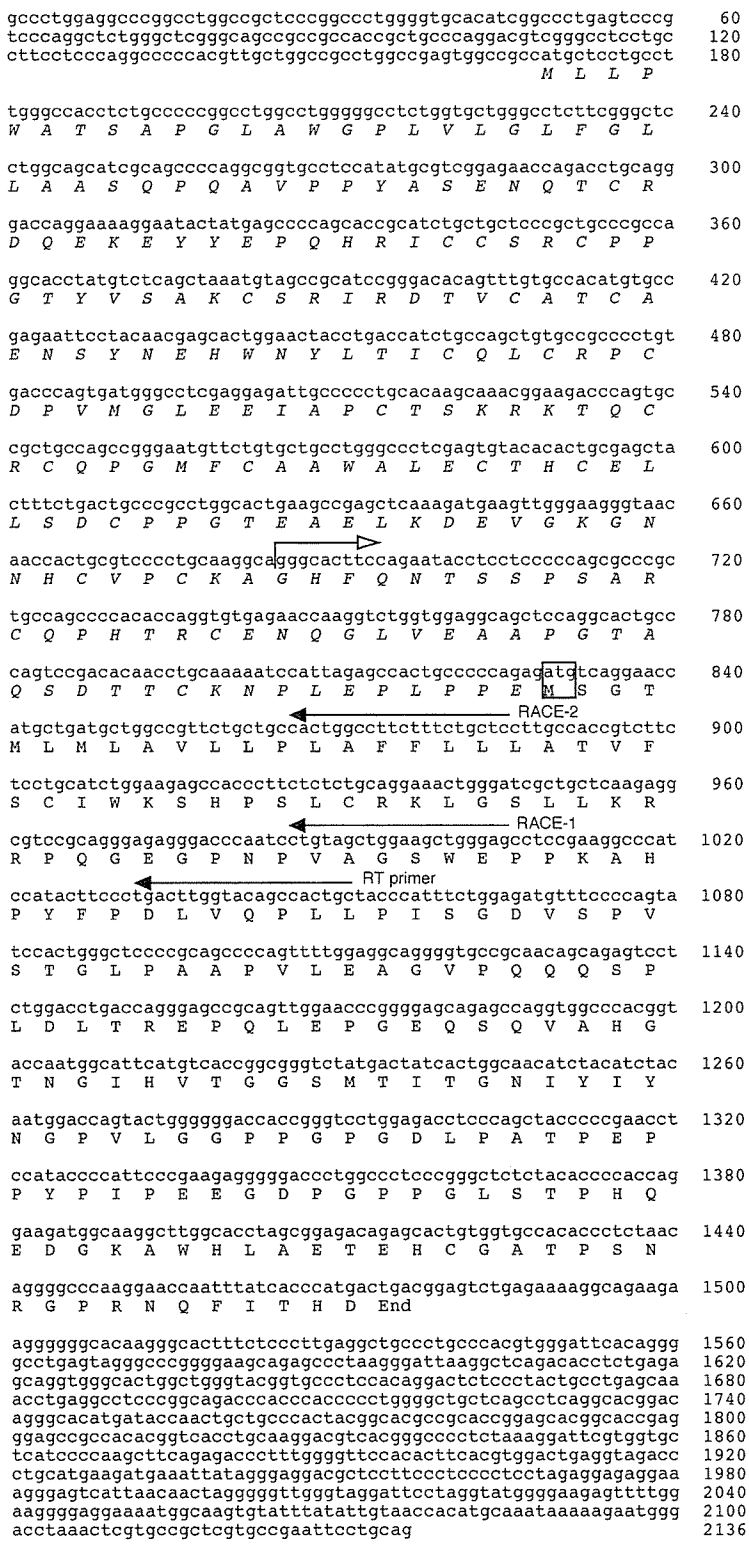

Fig. 2. Characterization of an LTBR cDNA isolated by screening for transformation activity. Amino acid residues of the full-length LTBR protein are aligned with the previously determined nucleotide sequence of LTBR cDNA (NM_002342). The cDNA isolated in the present study begins at nucleotide position 685 (open arrow) of the reported cDNA. The putative translation start site for the truncated (short-type) LTBR protein is boxed. The positions of primers used for 5′-RACE are indicated by closed arrows.

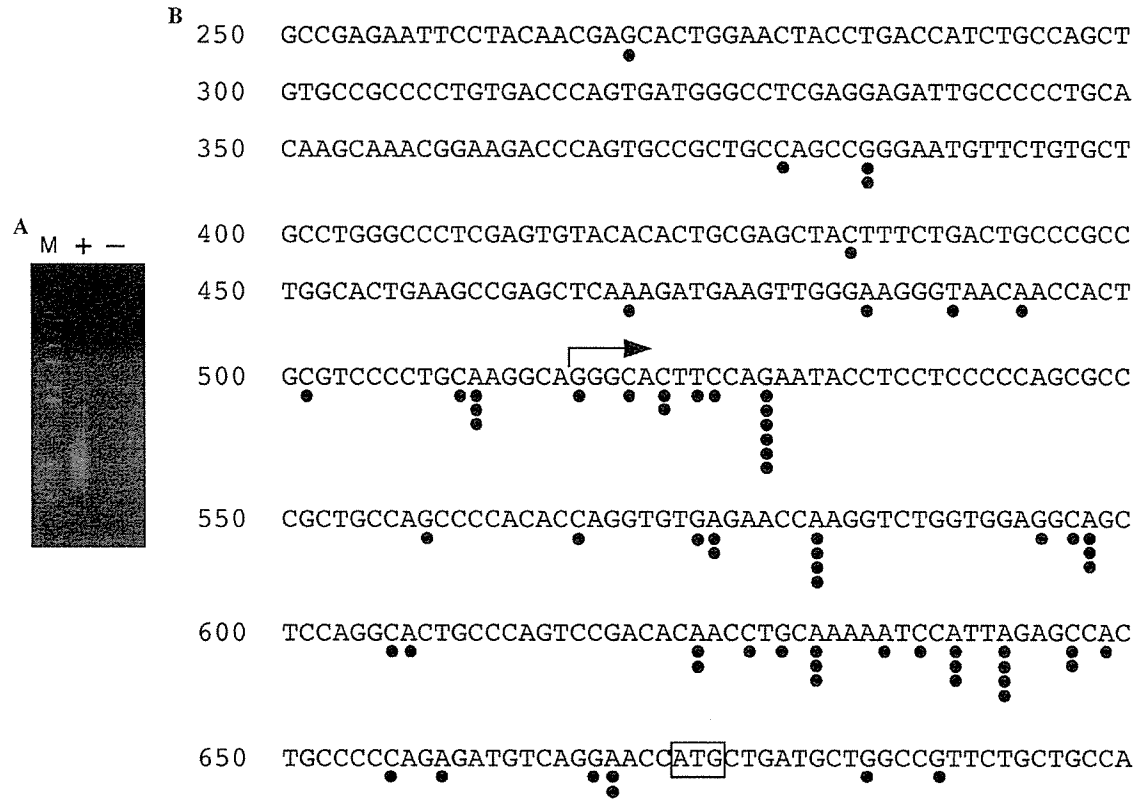

Fig. 3. 5′-RACE analysis of LTBR cDNA. (A) Total RNA of MiaPaCa-2 cells was incubated with the LTBR-specific RT primer in the presence (+) or absence (–) of reverse transcriptase, and resulting cDNA was subjected to PCR-based 5′-RACE. The PCR products were fractionated by electrophoresis through a 1.8% agarose gel and stained with ethidium bromide. Lane M, 1-kb DNA ladder. (**B**) The positions of the 5′ ends of 5′-RACE products are indicated by closed circles in alignment with the reported LTBR cDNA sequence. Numbers on the left indicate nucleotide positions relative to the translation initiation site of the full-length (wild-type) cDNA. The arrow indicates the 5′ end of the cDNA isolated by retroviral screening in the present study; the putative translation start codon of this cDNA is boxed.

human protein. The infected cells generated both transformed foci in vitro and tumors in nude mice (Fig. 5).

Discussion

In the present study, we constructed a retroviral cDNA expression library for a PDC cell line. Given that 80% (24/30) of the viral plasmids contained cDNA inserts and that the overall clone number was >1 million, this library should represent most of the mRNAs in MiaPaCa-2 cells. We infected 3T3 mouse fibroblasts with this recombinant library to screen for transforming genes with a focus formation assay. This screen identified *KRAS2* with an activating mutation as a transforming gene of MiaPaCa-2 cells, supporting the fidelity of our approach.

Our screen also identified a transforming cDNA that encodes an NH_2-terminally truncated form of LTBR. 5′-RACE analysis revealed the existence of mRNAs for this short-type LTBR in MiaPaCa-2 cells, and retrovirus-mediated expression of the isolated cDNA in 3T3 cells conferred the ability to grow in soft agar in vitro as well as the ability to form tumors in vivo.

LTBR belongs to the tumor necrosis factor (TNF) receptor superfamily [9] and binds two functional ligands, lymphotoxin-$\alpha 1\beta 2$ and LIGHT [10,11]. LTBR is expressed by many cell types (but not by lymphocytes), whereas expression of the LTBR ligands is restricted to activated lymphocytes [11]. Signaling by LTBR is important in the development of lymphoid tissue and in generation of adaptive humoral immune responses [12,13]. In general, LTBR function is thought to be linked to apoptosis. Indeed, activation of LTBR by its endogenous ligands or by anti-receptor antibodies triggers the death of various tumor cell lines [14,15]. Activation of the LIGHT-LTBR signaling pathway in tumor cells also induces marked chemokine-dependent recruitment of T cells to tumors, resulting in the rejection of established tumor cells [16].

LTBR activation has also been linked to tumor development, however. Its activation in fibrosarcoma cells thus induces angiogenesis and tumor growth by triggering the release of macrophage inflammatory protein-2, an angiogenic CXC chemokine [17]. Although oncogenic potential has not previously been demonstrated for LTBR, our data now show that both the full-length and truncated forms of this protein possess transforming activity even in the absence of exogenous cognate ligands. A high level of expression of LTBR conferred by the retroviral long terminal repeat in our experiments might have resulted in self-oligomerization

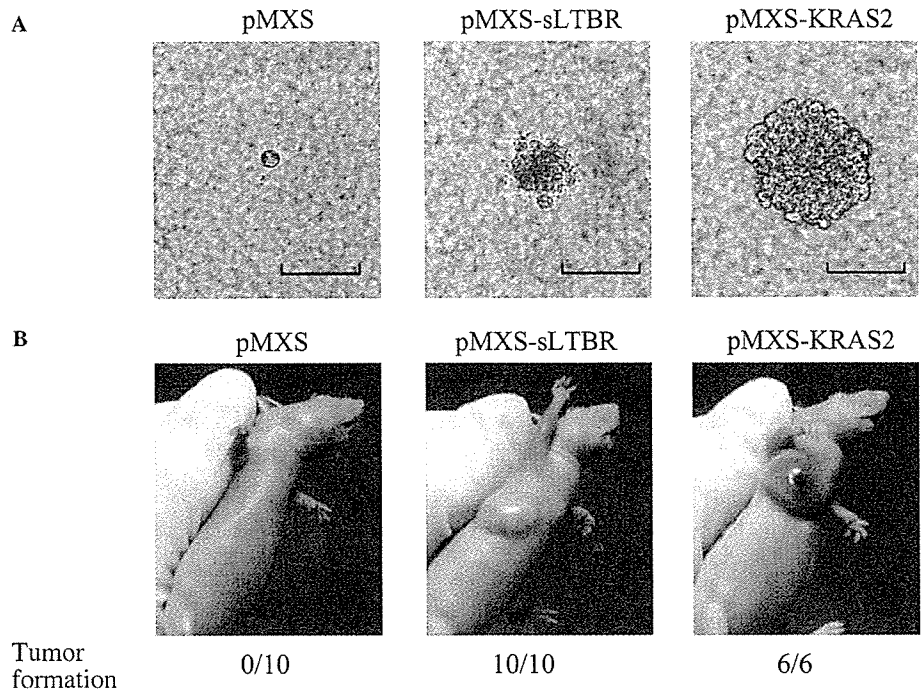

Fig. 4. Transforming activity of short-type LTBR. (A) Focus formation assay. 3T3 cells infected either with empty retrovirus (pMXS) or with retroviruses encoding short-type LTBR (pMXS-sLTBR) or activated KRAS2 (pMXS-KRAS2) were seeded into soft agar and incubated for 2 weeks. Scale bars, 100 μm. (B) Tumorigenicity assay. Cells infected as in (A) were injected into the shoulder of nude mice and tumor formation was examined after 3 weeks. The frequency of tumor formation determined is indicated.

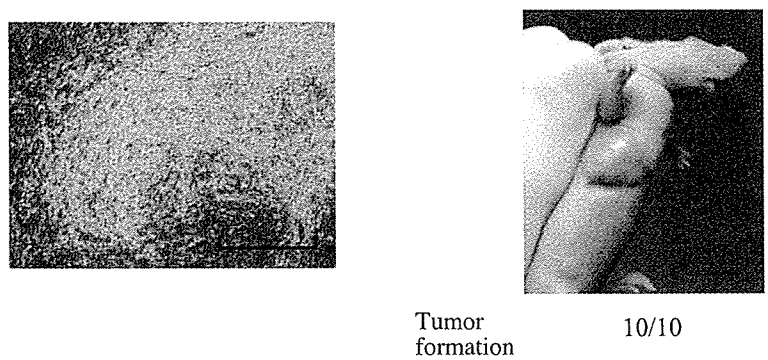

Fig. 5. Transforming activity of full-length LTBR. The transforming activity of a retroviral vector encoding full-length (wild-type) LTBR was evaluated by the focus formation assay (left) or the in vivo tumorigenicity assay (right). Scale bar, 1 mm.

of the protein. It is thus likely that LTBR exerts its oncogenic function in a tissue- and context-dependent manner. As shown here for PDC, it will be important to determine whether LTBR also contributes to the mechanism of transformation in other human malignancies.

Acknowledgments

This work was supported in part by a grant for Third-Term Comprehensive Control Research for Cancer from the Ministry of Health, Labor, and Welfare of Japan as well as by a grant for "High-Tech Research Center" Project for Private Universities: Matching Fund Subsidy (2002–2006) from the Ministry of Education, Culture, Sports, Science and Technology of Japan.

References

[1] S. Rosewicz, B. Wiedenmann, Pancreatic carcinoma, Lancet 349 (1997) 485–489.
[2] P.C. Bornman, I.J. Beckingham, Pancreatic tumours, Br. Med. J. 322 (2001) 721–723.
[3] M. Tada, M. Omata, M. Ohto, Clinical application of ras gene mutation for diagnosis of pancreatic adenocarcinoma, Gastroenterology 100 (1991) 233–238.
[4] S.R. Bramhall, The use of molecular technology in the differentiation of pancreatic cancer and chronic pancreatitis, Int. J. Pancreatol. 23 (1998) 83–100.

[5] G. Schneider, J.T. Siveke, F. Eckel, R.M. Schmid, Pancreatic cancer: basic and clinical aspects, Gastroenterology 128 (2005) 1606–1625.
[6] A. Yanagisawa, K. Ohtake, K. Ohashi, M. Hori, T. Kitagawa, H. Sugano, Y. Kato, Frequent c-Ki-ras oncogene activation in mucous cell hyperplasias of pancreas suffering from chronic inflammation, Cancer Res. 53 (1993) 953–956.
[7] S.A. Aaronson, Growth factors and cancer, Science 254 (1991) 1146–1153.
[8] M.A. Frohman, M.K. Dush, G.R. Martin, Rapid production of full-length cDNAs from rare transcripts: amplification using a single gene-specific oligonucleotide primer, Proc. Natl. Acad. Sci. USA 85 (1988) 8998–9002.
[9] P.D. Crowe, T.L. VanArsdale, B.N. Walter, C.F. Ware, C. Hession, B. Ehrenfels, J.L. Browning, W.S. Din, R.G. Goodwin, C.A. Smith, A lymphotoxin-β-specific receptor, Science 264 (1994) 707–710.
[10] J.L. Browning, I.D. Sizing, P. Lawton, P.R. Bourdon, P.D. Rennert, G.R. Majeau, C.M. Ambrose, C. Hession, K. Miatkowski, D.A. Griffiths, A. Ngam-ek, W. Meier, C.D. Benjamin, P.S. Hochman, Characterization of lymphotoxin-αβ complexes on the surface of mouse lymphocytes, J. Immunol. 159 (1997) 3288–3298.
[11] W.R. Force, B.N. Walter, C. Hession, R. Tizard, C.A. Kozak, J.L. Browning, C.F. Ware, Mouse lymphotoxin-β receptor. Molecular genetics, ligand binding, and expression, J. Immunol. 155 (1995) 5280–5288.
[12] A. Futterer, K. Mink, A. Luz, M.H. Kosco-Vilbois, K. Pfeffer, The lymphotoxin β receptor controls organogenesis and affinity maturation in peripheral lymphoid tissues, Immunity 9 (1998) 59–70.
[13] R.M. Locksley, N. Killeen, M.J. Lenardo, The TNF and TNF receptor superfamilies: integrating mammalian biology, Cell 104 (2001) 487–501.
[14] J.L. Browning, K. Miatkowski, I. Sizing, D. Griffiths, M. Zafari, C.D. Benjamin, W. Meier, F. Mackay, Signaling through the lymphotoxin β receptor induces the death of some adenocarcinoma tumor lines, J. Exp. Med. 183 (1996) 867–878.
[15] I.A. Rooney, K.D. Butrovich, A.A. Glass, S. Borboroglu, C.A. Benedict, J.C. Whitbeck, G.H. Cohen, R.J. Eisenberg, C.F. Ware, The lymphotoxin-β receptor is necessary and sufficient for LIGHT-mediated apoptosis of tumor cells, J. Biol. Chem. 275 (2000) 14307–14315.
[16] P. Yu, Y. Lee, W. Liu, R.K. Chin, J. Wang, Y. Wang, A. Schietinger, M. Philip, H. Schreiber, Y.X. Fu, Priming of naive T cells inside tumors leads to eradication of established tumors, Nat. Immunol. 5 (2004) 141–149.
[17] T. Hehlgans, B. Stoelcker, P. Stopfer, P. Muller, G. Cernaianu, M. Guba, M. Steinbauer, S.A. Nedospasov, K. Pfeffer, D.N. Mannel, Lymphotoxin-β receptor immune interaction promotes tumor growth by inducing angiogenesis, Cancer Res. 62 (2002) 4034–4040.

HUMAN GENE THERAPY 16:1212–1218 (October 2005)

Technical Report

Large-Scale Production of Recombinant Viruses by Use of a Large Culture Vessel with Active Gassing

TAKASHI OKADA,[1] TATSUYA NOMOTO,[1] TORU YOSHIOKA,[1] MUTSUKO NONAKA-SARUKAWA,[1] TAKAYUKI ITO,[1] TSUYOSHI OGURA,[1] MAYUMI IWATA-OKADA,[2] RYOSUKE UCHIBORI,[1] KUNIKO SHIMAZAKI,[3] HIROAKI MIZUKAMI,[1] AKIHIRO KUME,[1] and KEIYA OZAWA[1,2]

ABSTRACT

Adenovirus and adeno-associated virus (AAV) vectors are increasingly used for gene transduction experiments. However, to produce a sufficient amount of these vectors for *in vivo* experiments requires large-capacity tissue culture facilities, which may not be practical in limited laboratory space. We describe here a large-scale method to produce adenovirus and AAV vectors with an active gassing system that uses large culture vessels to process labor- and cost-effective infection or transfection in a closed system. Development of this system was based on the infection or transfection of 293 cells on a large scale, using a large culture vessel with a surface area of 6320 cm^2. A minipump was connected to the gas inlet of the large vessel, which was placed inside the incubator, so that the incubator atmosphere was circulated through the vessel. When active gassing was employed, the productivity of the adenovirus and AAV vectors significantly increased. This vector production system was achieved by improved CO_2 and air exchange and maintenance of pH in the culture medium. Viral production with active gassing is particularly promising, as it can be used with existing incubators and the large culture vessel can readily be converted for use with the active gassing system.

OVERVIEW SUMMARY

Large-scale production of recombinant viruses, using a large culture vessel with active gassing, is superior to protocols using standard tissue culture plates or flasks because of the higher capacity for cell growth. Although a previous protocol for recombinant virus production in a large culture vessel had the problem of insufficient transduction efficiency resulting from inadequate gas exchange, a method to use active gassing successfully improved productivity of recombinant viruses. Development of a vector production system on a large scale, using commercially available large culture vessels, allows us to process labor- and cost-effective manipulation in a closed system.

INTRODUCTION

ADENOVIRUS AND ADENO-ASSOCIATED VIRUS (AAV) VECTORS are highly efficient for transduction in many gene therapy studies (Okada *et al.*, 2002b, 2004; Ito *et al.*, 2003; Nomoto *et al.*, 2003; Yamaguchi *et al.*, 2003; Mochizuki *et al.*, 2004; Yoshioka *et al.*, 2004; Liu *et al.*, 2005). However, current production methods rely on the manipulation of many individual flasks and are not generally considered appropriate for scaling-up of production because it would be a time-consuming and labor-intensive process. Therefore, alternative tissue culture vessels with higher capacity for cell growth, such as a 10-tray Cell Factory (CF10; Nalge Nunc International, Rochester, NY) with a surface area of 6320 cm^2, could be suitable for scaling-up of

[1]Division of Genetic Therapeutics, Center for Molecular Medicine, Jichi Medical School, Tochigi 329-0498, Japan.
[2]Division of Hematology, Department of Medicine, Jichi Medical School, Tochigi 329-0498, Japan.
[3]Department of Physiology, Jichi Medical School, Tochigi 329-0498, Japan.

vector production (Okada *et al.*, 2002a). This device is easy to handle and can be used for efficient cell culture on a large scale in a closed system requiring only an air filter (Berger *et al.*, 2002; Tuyaerts *et al.*, 2002). Nevertheless, a previous protocol for recombinant virus production in the CF10 had the problem of insufficient scaling-up of vector production (Liu *et al.*, 2003). In that protocol, inadequate gas exchange between the culture vessel and the incubator might have been the cause of the inefficient yield.

We consequently adapted an active gassing system to generate large numbers of recombinant viruses in the CF10. The purpose of this active gassing is to control and maintain CO_2 tension and pH in the growth medium by passing a gas mixture through the CF10. For many types of cells, pH is an important parameter for controlling cell growth. This can be achieved by gassing with CO_2 in atmospheric air in the incubator. Enhanced gas exchange in a large culture vessel should improve both viral infectivity and plasmid transfection efficiency. In combination with the previously described method of using the CF10 (Okada *et al.*, 2002a), we have now created a simple and highly efficient system of producing vector stock on a large scale. Presented here is a labor- and cost-effective method for large-scale production of adenovirus and AAV vectors with an active gassing system that uses a large culture vessel to achieve transfection or infection in a closed system.

MATERIALS AND METHODS

Cell culture with active gassing

Propagation of vectors was based on the infection or transfection of human embryonic kidney-derived 293B cells (Yamaguchi *et al.*, 2003) by using either a flask with a surface area of 225 cm^2 (Falcon, T-225; BD Biosciences Discovery Labware, Bedford, MA) or the CF10, as described previously (Okada *et al.*, 2002a). Cells were cultured in Dulbecco's modified Eagle's medium and nutrient mixture F12 (DMEM–F12: Invitrogen, Grand Island, NY) with 10% fetal bovine serum (FBS; Sigma-Aldrich, St. Louis, MO), penicillin (100 units/ml), and streptomycin (100 μg/ml) at 37°C in a 5% CO_2 incubator. First, cells were plated at 2.3×10^6 cells per T-225 or at 6.5×10^7 cells per CF10 to achieve a monolayer at 20 to 40% confluency when cells initially attach to the surface of the flask. The volume of medium used per flask was 40 ml per T-225 or 1120 ml per CF10. Subsequently, cells were grown to a confluency of 70–90% over the next 48 to 72 hr for adenovirus infection or plasmid transfection. An aquarium pump (NISSO, Tokyo, Japan) was used to circulate air through the CF10 with 5% CO_2 and humidity control by an incubator. The CF10 was mounted with a bacterial air filter (bacterial air vents; Pall Gelman Sciences, Ann Arbor, MI) to connect the aquarium pump. The pump was connected to the gas inlet of the CF10 and the CF10 was placed inside the incubator, so that the incubator atmosphere was circulated through the CF10. The flow through the CF10 was maintained at 500 ml/min. Culture medium was sampled periodically, and the CO_2 concentrations and pH were estimated with a blood gas analyzer (Nova PHOX; Diamond Diagnostics, Holliston, MA). Glucose levels of the culture medium were also estimated with a glucose meter (Glutest Sensor, Glutest Ace GT-1640; Sanwa Kagaku Kenkyusho, Nagoya, Japan).

Construction and propagation of adenoviral vectors

A recombinant adenoviral vector, Ad-EGFP, was constructed using an adenoviral DNA–protein complex without a transgene insert (AVC2.null) (Okada *et al.*, 1998); it carried the cytomegalovirus (CMV) promoter, cloning sites, a simian virus 40 (SV40) intron, and the SV40 polyadenylation signal. To generate Ad-EGFP encoding enhanced green fluorescent protein (EGFP), a *Spe*I–*Cla*I fragment containing the *EGFP* cDNA excised from pEGFP-1 (BD Biosciences Clontech, Palo Alto, CA) was inserted into the *Xba*I and *Nsp*V sites in the DNA–protein complex, AVC2.null, using the direct *in vitro* ligation technique (Okada *et al.*, 1998). The ligated DNA–protein complex was introduced into 293 cells by the calcium phosphate transfection method. Viral plaques on 293 cells were isolated, amplified, and titrated by standard techniques. To amplify the vector in 293 cells, half the medium in the tissue culture flasks was exchanged with fresh DMEM–F12 containing 10% FBS 1 hr before infection. Cells were infected with the virus at 10 multiplicities of infection (MOI) per cell. Cells were incubated to reach full cytopathic effect, and crude viral lysate was purified by two rounds of CsCl two-tier centrifugation. The average number of plaque-forming units (PFU) was assessed on the basis of the 50% tissue culture infective dose. The number of vector particles was estimated by dot-blot hybridization of DNase I-treated stocks with plasmid standards.

Construction and propagation of AAV vectors

AAV1-EGFP, a recombinant AAV type 1 expressing the *EGFP* gene under the control of the CAG promoter (modified chicken β-actin promoter) with the CMV-IE enhancer, was generated by the following procedure. A *Bam*HI–*Xba*I fragment containing EGFP cDNA excised from pEGFP-1 and a *Hin*dIII fragment containing the woodchuck hepatitis virus posttranscriptional regulatory element (WPRE) sequence excised from pBluescript II SK(+)WPRE-B11 (a gift from T. Hope, University of Illinois at Chicago, Chicago, IL) was cloned into an *Xho*I site of pCAGGS (a gift from J.-i. Miyazaki, Osaka University Graduate School of Medicine, Japan) to create pCAG-EGFP-WPRE, using an *Xho*I linker. The EGFP expression cassette in pCAG-EGFP-WPRE was ligated to *Not*I-excised pAAV-LacZ to form the proviral vector plasmid pAAV2-CAG-EGFP-WPRE. AAV viral stocks were prepared according to a previously described protocol (Okada *et al.*, 2002a) with minor modifications. Half the medium in tissue culture flasks was exchanged with fresh DMEM–F12 containing 10% FBS 1 hr before plasmid transfection. Subsequently, cells were cotransfected with 23 μg (per T-225) or 650 μg (per CF10) of each of the following plasmids: a proviral vector plasmid, AAV-1 chimeric helper plasmid p1RepCap (Mochizuki *et al.*, 2004), and adenoviral helper plasmid pAdeno, by a calcium phosphate coprecipitation method. Each of the vector and helper plasmids was added to 4 ml (per T-225) or 112 ml (per CF10) of 300 m*M* $CaCl_2$. This solution was gently added to an equal volume of 2× HEPES-buffered saline (HBS: 290 m*M* NaCl, 50 m*M* HEPES buffer, 1.5 m*M* Na_2HPO_4, pH 7.0) and immediately mixed by gentle inversion three times to form a uniform solution. This solution was immediately mixed with fresh DMEM–F12 containing 10% FBS outside the flasks to produce a homogeneous plasmid solution mixture. Subsequently, medium in the

culture flasks was entirely replaced with this plasmid solution mixture. At the end of incubation for 6 hr, the plasmid solution mixture in the culture flasks was replaced with prewarmed fresh DMEM–F12 containing 2% FBS. Cell suspensions were collected 72 hr after transfection and centrifuged at 300 × *g* for 10 min. Each cell pellet was resuspended in 2 ml (per T-225) or 56 ml (per CF10) of Tris-buffered saline (TBS: 100 m*M* Tris-HCl [pH 8.0], 150 m*M* NaCl). Recombinant AAV was harvested by three cycles of freeze–thawing of each resuspended pellet. Crude viral lysate was then purified twice by passage through a CsCl two-tier centrifugation gradient, as described previously (Okada *et al.*, 2002b). The viral stock was titrated by dot-blot hybridization of DNase I-treated stocks with plasmid standards. To confirm transgene expression with the propagated vector *in vivo*, 5-week-old male Sprague-Dawley rats were injected via the anterior tibial muscle with AAV1-EGFP (1×10^{11} genome copies per rat). Fifteen weeks after injection, the rats were sacrificed and expression was confirmed by fluorescence microscopy.

Statistical analysis

Statistical significance was determined on the basis of an unpaired, two-tailed p value and Student t test, and a p value less than 0.05 was considered significant.

RESULTS

Improved gas exchange and maintenance of pH in medium after recombinant adenovirus infection

Propagation of vectors was based on infection or transfection of 293 cells on a large scale. A minipump was connected to the gas inlet of the CF10 and placed inside the incubator, so that the atmosphere in the incubator, containing 5% CO_2, was circulated through the CF10. The gas flow for circulation through the CF10 was maintained at 500 ml/min. An appropriate gas flow rate was important to give a uniform distribution of the gas in the individual trays of the CF10. A flow less than 200 ml/min gave uneven distribution of the gas, and significantly influenced cell growth. Gas flow that was too high also disturbed the uniformity of cell density. Appropriate cell density and uniform distribution of cells are critical to achieve successful gene transduction. Application of active gassing significantly increased cell growth in the CF10 (Table 1). CO_2 concentrations in the media stayed at their initial levels when using either a T-225 or CF10 with active gassing (Fig. 1A). In contrast, the CO_2 concentration inside the CF10 increased subsequent to adenovirus infection in the absence of active gassing. The pH of culture medium in the CF10 with active gassing was close to that in the T-225 and significantly higher than that in the CF10 without active gassing (Fig. 1B).

Monitoring of cell numbers and time point for harvest

The glucose level was monitored as an index for tracing cell growth and cytopathic effect in the CF10 to avoid the necessity for a specialized microscope to monitor cells in the large culture vessel. The glucose level decreased with increasing cell confluency and progression of cytopathic effect (CPE) (Fig. 2). When 80% CPE was reached, the glucose level was reduced to about 50 mg/ml. When glucose levels were less than 25%, the cells showed full CPE and this was regarded as the appropriate time for harvest.

Improved adenovirus vector production in a large culture vessel with active gassing

We estimated the adenovirus vector yield propagated by using 28 T-225 flasks with a surface area of 225 cm^2, a CF10 with a surface area of 6320 cm^2, or a CF10 in the presence of active gassing. When active gassing was used with the CF10, the productivity of the adenovirus vectors was dramatically increased, by 53.4 times compared with that in the CF10 without active gassing (Fig. 3). The vector yield per producer cell in the CF10 was also significantly improved in the presence of active gassing (Table 1). The PFU-to-particle ratios for vectors produced in the T-225, CF10, and CF10 with active gassing were 1:7, 1:15, and 1:10, respectively.

Efficient AAV vector production in a large culture vessel with active gassing

Enhanced gas exchange in a large culture vessel should also improve vector production through plasmid transfection. AAV vectors were produced in a large vessel by a three-plasmid transfection adenovirus-free protocol (Okada *et al.*, 2002b). Three days after plasmid transfection, the CO_2 concentrations in medium from the CF10 in the presence of active gassing were significantly less than those without active gassing (Table 2). The pH of the culture medium in the CF10 with active gassing was also improved. The CF-10 with active gassing was compatible with the three-plasmid transfection protocol for recombinant AAV production. When we used active gassing, the vec-

TABLE 1. INCREASED CELL GROWTH AND VECTOR YIELD WITH ACTIVE CO_2 AND AIR EXCHANGE[a]

Flask	*Number of cells harvested*	*Vector yield per cell (PFU/cell)*
225-cm^2 flask	$(1.4 \pm 0.2) \times 10^9$ (per 28 flasks)	7.9×10^3
CF10	$(4.9 \pm 1.6) \times 10^8$	4.1×10^2
CF10 + AG	$(1.3 \pm 0.3) \times 10^9$	8.2×10^3

[a]At the time of cell harvest after adenovirus infection, cell growth and vector yield per cell in a CF10 with a surface area of 6320 cm^2 in the presence or absence of active gassing (AG) were compared with that in 28 flasks with a surface area of 225 cm^2 each.

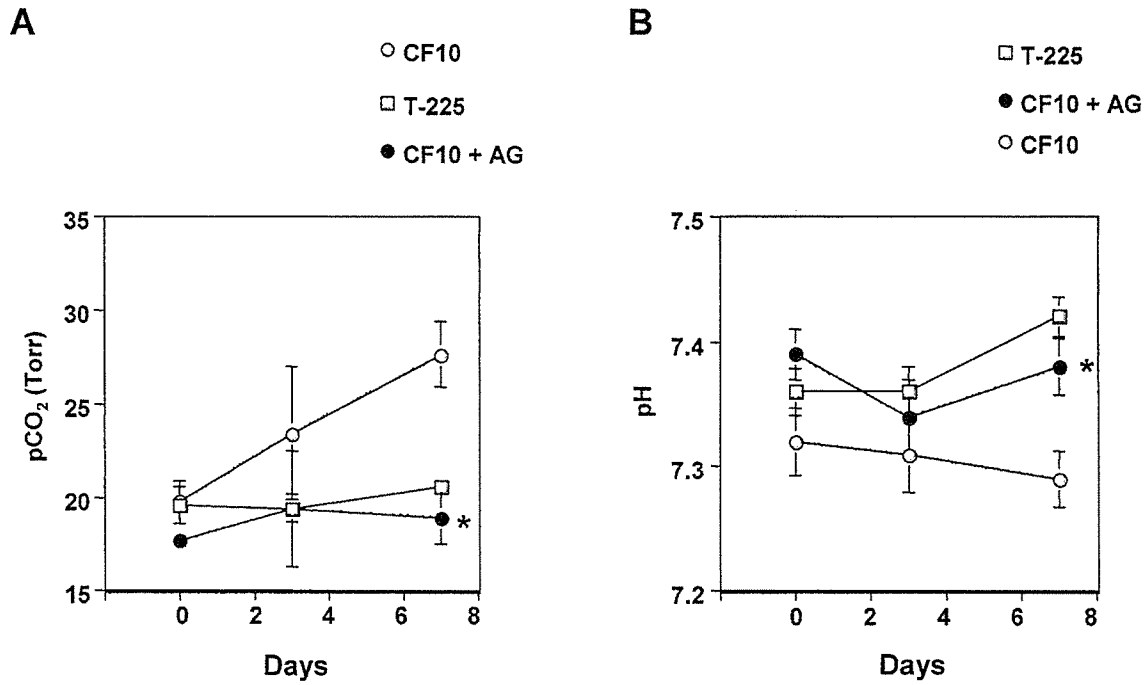

FIG. 1. Improved CO_2 and air exchange and maintenance of pH in conditioned medium after recombinant adenovirus infection. Subsequent to adenovirus infection in a normal flask with a surface area of 225 cm^2 (T-225) or a large culture vessel (a 10-tray Cell Factory [CF10] with a surface area of 6320 cm^2) in the presence or absence of active gassing (AG), CO_2 concentrations (**A**) and pH (**B**) in conditioned medium were determined ($n = 4$). Asterisk indicates $p < 0.05$ in comparison with a CF10 without AG.

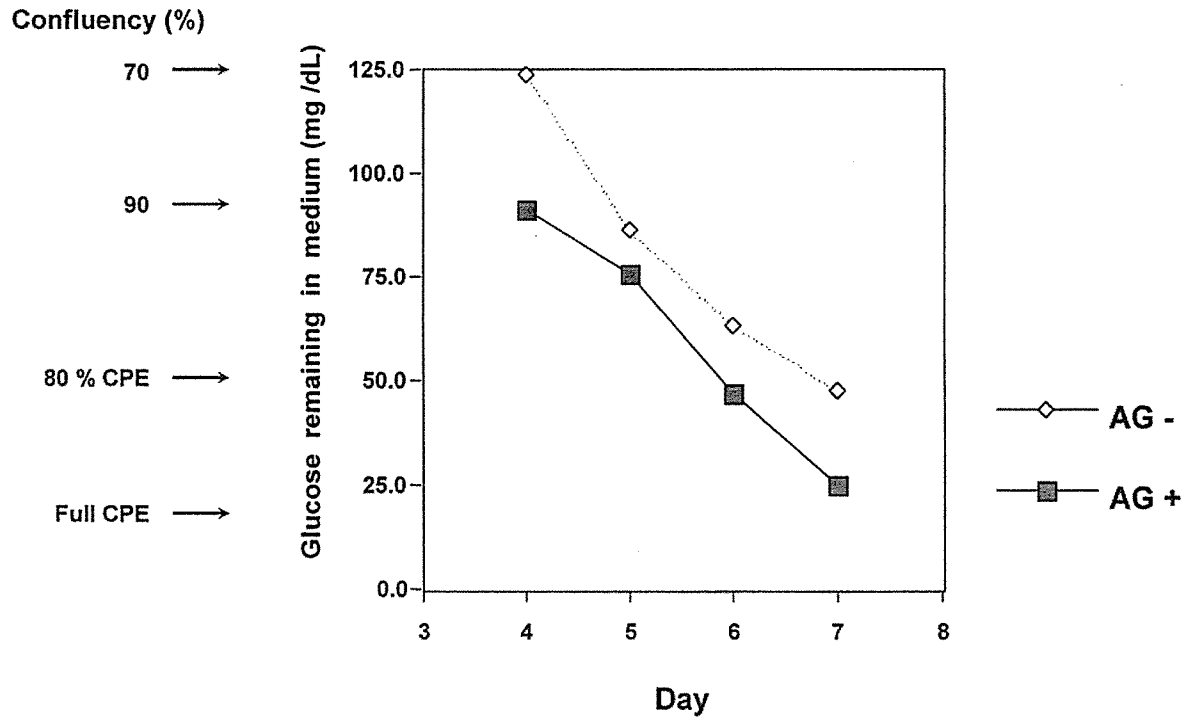

FIG. 2. Glucose reading to monitor cell growth. Glucose reading of culture medium was used as an index to monitor cell growth and cytopathic effect (CPE) in the CF10 to avoid the need for a specialized microscope. Cells were infected with recombinant adenovirus in the presence or absence of active gassing (AG) when 90% confluent.

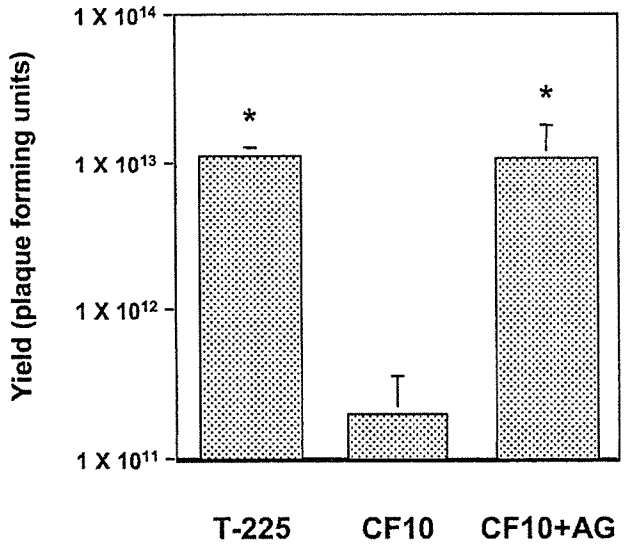

FIG. 3. Improved production of adenovirus vector. Adenovirus vector was propagated in 28 T-225 flasks ($n = 4$), a CF10 ($n = 3$), or a CF10 in the presence of active gassing (CF10 + AG, $n = 3$). Adenovirus vector expressing an EGFP reporter gene was generated in two independent experiments. The average number of plaque-forming units (PFU) was assessed by $TCID_{50}$. $*p < 0.05$ in comparison with a CF10 without AG.

tor yield per cell was increased significantly, by 3.5 times (Table 3). Although vector yield was dependent on the transgene and construct, production of vector particles at up to 2.0×10^{13} genome copies per CF-10 was achieved.

Transduction of muscles with AAV vectors produced in a large culture vessel with active gassing

Five-week-old male Sprague-Dawley rats were injected with AAV1-enhanced green fluorescence protein (EGFP) (1×10^{11} genome copies per rat) via the anterior tibial muscle. Fifteen weeks after injection, the rats were sacrificed to confirm expression by fluorescence microscopy. The injected sites showed efficient expression of EGFP (Fig. 4).

TABLE 2. ENHANCED GAS EXCHANGE AND MAINTENANCE OF pH IN CONDITIONED MEDIUM AFTER PLASMID TRANSFECTION[a]

	pCO_2 (Torr)	*pH*
CF10	25.6 ± 1.1	7.23 ± 0.03
CF10 + AG	14.2 ± 0.1	7.40 ± 0.01

[a]Three days after plasmid transfection by using CF10 in the presence or absence of active gassing (AG), CO_2 concentrations and pH in the conditioned medium were estimated. Means ± standard deviations are shown ($n = 4$).

TABLE 3. IMPROVED YIELDS OF RECOMBINANT AAV TYPE 1 BY ACTIVE GAS EXCHANGE[a]

	Yield per vessel	*Yield per cell*
CF10	$(2.2 \pm 0.5) \times 10^{12}$	$(3.1 \pm 0.6) \times 10^{3}$
CF10 ± AG	$(1.0 \pm 0.7) \times 10^{13}$	$(1.1 \pm 0.7) \times 10^{4}$

[a]Titers of AAV1-EGFP were determined as genome copies by dot-blot analysis of DNase-treated stocks. AG, active gassing. Means ± standard deviations are shown ($n = 4$).

DISCUSSION

Successful vector production in a large culture vessel was achieved by improvement of CO_2 and air exchange along with maintenance of pH in the medium. Adenovirus production was enhanced by more than 50 times with the active gassing sys-

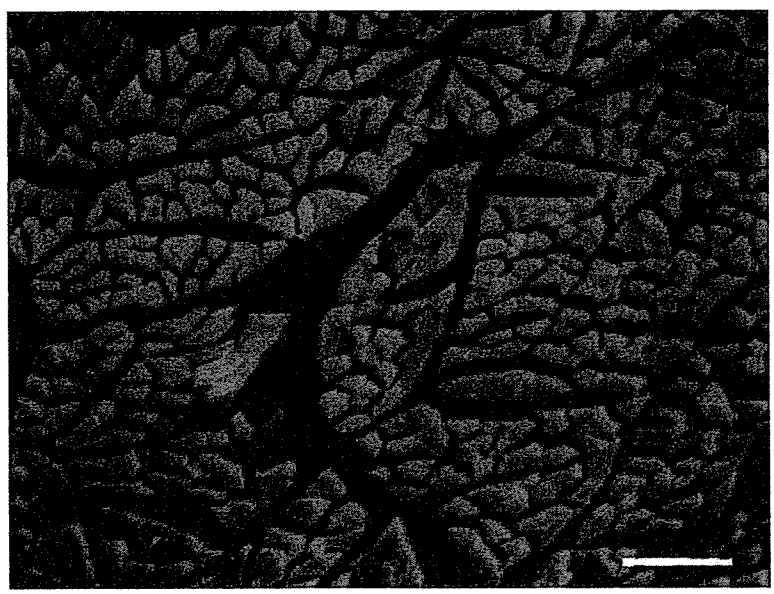

FIG. 4. Transduction of muscles with AAV vectors *in vivo*. Five-week-old male Sprague-Dawley rats were injected with AAV1-EGFP (1×10^{11} genome copies per body) via the anterior tibial muscle. Fifteen weeks after injection, the rats were killed to confirm expression by fluorescence microscopy. Scale bar: 100 μm.

tem. CF-10 with active gassing was also compatible with the three-plasmid transfection protocol for recombinant AAV production. When we used active gassing, the productivity of the AAV vectors was significantly increased.

In a direct comparison with vectors generated in ordinary culture flasks, viruses from the CF10 with active gassing were equivalent regarding function and bioactivity. The use of a CF10 with active gassing thus resulted in the production of vectors equivalent to those obtained in conventional culture dishes, but with a dramatically reduced workload. An average yield of approximately 1.0×10^{13} PFU requires as many as 28 T-225 flasks, according to our previous protocol. Alternatively, only one CF10 with active gassing was enough to achieve the same amount of virus. Furthermore, the PFU-to-particle ratio was also increased with the use of active gassing, suggesting improved bioactivity of the viruses. We used this system to amplify various adenovirus vectors. Although vector yield was dependent on the transgene and construct, a proportional increase in yield relative to surface area was achieved (data not shown).

The system was also compatible with plasmid transfection for recombinant AAV production. Active gassing combined with a large culture vessel significantly increased the productivity of the AAV vectors. The effect of enhanced gas exchange on the productivity of AAV vectors was less than the effect on the productivity of adenovirus vectors. Because lactate production accompanied by adenovirus replication is much greater than that with AAV, the protection of cells against pH drop by maintaining the CO_2 tension might be a plausible explanation for the preferential effect on adenovirus production. Transient transfection in a large culture vessel also provides a simple and flexible method of producing lentivirus-based vectors (Karolewski *et al.*, 2003). Therefore, our protocol would also be applicable to the efficient production of lentivirus- or retrovirus-based vectors.

Because this system fits into existing incubators and current vessels can readily be converted to the active gassing system, the viral production protocol using a CF-10 coupled with active gassing has practical utility for growing recombinant virus stocks in a limited laboratory space. This system has proven successful in our repeated manipulations and appears particularly promising. We have used the CF10 with the active gassing system in more than 400 vector preparations in the course of our more recent gene therapy experiments. The system allows us to perform a considerable number of *in vivo* experiments and to validate our studies.

ACKNOWLEDGMENTS

The authors thank Dr. Villy Nielsen, Ph.D. (Nunc, Roskilde, Denmark) and Mr. Hiroyuki Sano (Nalge Nunc International, Japan) for helpful discussions. We thank Avigen (Alameda, CA) for providing pAAV-LacZ and pAdeno. We thank Dr. Thomas Hope (University of Illinois at Chicago) for providing pBluescript II SK(+)WPRE-B11 and Dr. Jun-ichi Miyazaki (Osaka University Graduate School of Medicine, Japan) for pCAGGS. We also thank Ms. Miyoko Mitsu and Mr. Masataka Takahashi (Ieda Chemicals, Japan) for their encouragement and technical support. This study was supported in part by grants from the Ministry of Health, Labor, and Welfare of Japan; Grants-in-Aid for Scientific Research; a grant for the 21st Century Center of Excellence Program; and a matching fund subsidy from the High-Tech Research Center Project for Private Universities, through the Ministry of Education, Culture, Sports, Science, and Technology of Japan.

REFERENCES

BERGER, T.G., FEUERSTEIN, B., STRASSER, E., HIRSCH, U., SCHREINER, D., SCHULER, G., and SCHULER-THURNER, B. (2002). Large-scale generation of mature monocyte-derived dendritic cells for clinical application in cell factories. J. Immunol. Methods **268,** 131–140.

ITO, A., OKADA, T., MIZUGUCHI, H., HAYAKAWA, T., MIZUKAMI, H., KUME, A., TAKATOKU, M., KOMATSU, N., HANAZONO, Y., and OZAWA, K. (2003). A soluble CAR–SCF fusion protein improves adenoviral vector-mediated gene transfer to c-Kit-positive hematopoietic cells. J. Gene Med. **5,** 929–940.

KAROLEWSKI, B.A., WATSON, D.J., PARENTE, M.K., and WOLFE, J.H. (2003). Comparison of transfection conditions for a lentivirus vector produced in large volumes. Hum. Gene Ther. **14,** 1287–1296.

LIU, Y., OKADA, T., SHEYKHOLESLAMI, K., SHIMAZAKI, K., NOMOTO, T., MURAMATSU, S., KANAZAWA, T., TAKEUCHI, K., AJALLI, R., MIZUKAMI, H., KUME, A., ICHIMURA, K., and OZAWA, K. (2005). Specific and efficient transduction of cochlear inner hair cells with recombinant adeno-associated virus type 3 vector. Mol. Ther. (in press).

LIU, Y.L., WAGNER, K., ROBINSON, N., SABATINO, D., MARGARITIS, P., XIAO, W., and HERZOG, R.W. (2003). Optimized production of high-titer recombinant adeno-associated virus in roller bottles. Biotechniques **34,** 184–189.

MOCHIZUKI, S., MIZUKAMI, H., KUME, A., MURAMATSU, S., TAKEUCHI, K., MATSUSHITA, T., OKADA, T., KOBAYASHI, E., HOSHIKA, A., and OZAWA, K. (2004). Adeno-associated virus (AAV) vector-mediated liver- and muscle-directed transgene expression using various kinds of promoters and serotypes. Gene Ther. Mol. Biol. **8,** 9–18.

NOMOTO, T., OKADA, T., SHIMAZAKI, K., MIZUKAMI, H., MATSUSHITA, T., HANAZONO, Y., KUME, A., KATSURA, K., KATAYAMA, Y., and OZAWA, K. (2003). Distinct patterns of gene transfer to gerbil hippocampus with recombinant adeno-associated virus type 2 and 5. Neurosci. Lett. **340,** 153–157.

OKADA, T., RAMSEY, W.J., MUNIR, J., WILDNER, O., and BLAESE, R.M. (1998). Efficient directional cloning of recombinant adenovirus vectors using DNA–protein complex. Nucleic Acids Res. **26,** 1947–1950.

OKADA, T., NOMOTO, T., SHIMAZAKI, K., LIJUN, W., LU, Y., MATSUSHITA, T., MIZUKAMI, H., URABE, M., HANAZONO, Y., KUME, A., MURAMATSU, S., NAKANO, I., and OZAWA, K. (2002a). Adeno-associated virus vectors for gene transfer to the brain. Methods **28,** 237–247.

OKADA, T., SHIMAZAKI, K., NOMOTO, T., MATSUSHITA, T., MIZUKAMI, H., URABE, M., HANAZONO, Y., KUME, A., TOBITA, K., OZAWA, K., and KAWAI, N. (2002b). Adeno-associated viral vector-mediated gene therapy of ischemia-induced neuronal death. Methods Enzymol. **346,** 378–393.

OKADA, T., CAPLEN, N.J., RAMSEY, W.J., ONODERA, M., SHIMAZAKI, K., NOMOTO, T., AJALLI, R., WILDNER, O., MORRIS, J., KUME, A., HAMADA, H., BLAESE, R.M., and OZAWA, K. (2004). *In situ* generation of pseudotyped retroviral progeny by adenovirus-mediated transduction of tumor cells enhances the killing effect of HSV-tk suicide gene therapy *in vitro* and *in vivo*. J. Gene Med. **6,** 288–299.

TUYAERTS, S., NOPPE, S.M., CORTHALS, J., BRECKPOT, K., HEIRMAN, C., DE GREEF, C., VAN RIET, I., and THIELEMANS,

K. (2002). Generation of large numbers of dendritic cells in a closed system using Cell Factories. J. Immunol. Methods **264,** 135–151.

YAMAGUCHI, T., OKADA, T., TAKEUCHI, K., TONDA, T., OHTAKI, M., SHINODA, S., MASUZAWA, T., OZAWA, K., and INABA, T. (2003). Enhancement of thymidine kinase-mediated killing of malignant glioma by BimS, a BH3-only cell death activator. Gene Ther. **10,** 375–385.

YOSHIOKA, T., OKADA, T., MAEDA, Y., IKEDA, U., SHIMPO, M., NOMOTO, T., TAKEUCHI, K., NONAKA-SARUKAWA, M., ITO, T., TAKAHASHI, M., MATSUSHITA, T., MIZUKAMI, H., HANAZONO, Y., KUME, A., OOKAWARA, S., KAWANO, M., ISHIBASHI, S., SHIMADA, K., and OZAWA, K. (2004). Adeno-associated virus vector-mediated interleukin-10 gene transfer inhibits atherosclerosis in apolipoprotein E-deficient mice. Gene Ther. **11,** 1772–1779.

Address reprint requests to:
Dr. Takashi Okada
Division of Genetic Therapeutics
Center for Molecular Medicine
Jichi Medical School
3311-1 Yakushiji
Minami-Kawachi, Tochigi 329-0498, Japan

E-mail: tokada@jichi.ac.jp

Received for publication May 17, 2005; accepted after revision August 8, 2005.

Published online: September 21, 2005.

doi:10.1016/j.ymthe.2005.03.021

ARTICLE

Specific and Efficient Transduction of *Cochlear* Inner Hair Cells with Recombinant Adeno-associated Virus Type 3 Vector

Yuhe Liu,[1,2] Takashi Okada,[1] Kianoush Sheykholeslami,[3] Kuniko Shimazaki,[4] Tatsuya Nomoto,[1] Shin-Ichi Muramatsu,[5] Takeharu Kanazawa,[6] Koichi Takeuchi,[7] Rahim Ajalli,[2] Hiroaki Mizukami,[1] Akihiro Kume,[1] Keiichi Ichimura,[2] and Keiya Ozawa[1,*]

[1]*Division of Genetic Therapeutics, Center for Molecular Medicine, Jichi Medical School, 3311-1 Yakushiji, Minami-kawachi, Kawachi, Tochigi 329-0498, Japan*
[2]*Department of Otolaryngology and Head and Neck Surgery, Jichi Medical School, 3311-1 Yakushiji, Minami-kawachi, Kawachi, Tochigi 329-0498, Japan*
[3]*Department of Neurobiology, Northeastern Ohio Universities College of Medicine, Rootstown, OH 44272, USA*
[4]*Department of Physiology, Jichi Medical School, 3311-1 Yakushiji, Minami-kawachi, Kawachi, Tochigi 329-0498, Japan*
[5]*Department of Medicine, Division of Neurology, Jichi Medical School, 3311-1 Yakushiji, Minami-kawachi, Kawachi, Tochigi 329-0498, Japan*
[6]*Department of Otolaryngology and Head and Neck Surgery, Faculty of Medicine, University of the Ryukyus, Okinawa 903-0213, Japan*
[7]*Department of Anatomy, Jichi Medical School, 3311-1 Yakushiji, Minami-kawachi, Kawachi, Tochigi 329-0498, Japan*

**To whom correspondence and reprint requests should be addressed. Fax: (+81) 285 44 8675. E-mail: kozawa@jichi.ac.jp.*

Available online 12 May 2005

Recombinant adeno-associated virus (AAV) vectors are of interest for cochlear gene therapy because of their ability to mediate the efficient transfer and long-term stable expression of therapeutic genes in a wide variety of postmitotic tissues with minimal vector-related cytotoxicity. In the present study, seven AAV serotypes (AAV1–5, 7, 8) were used to construct vectors. The expression of EGFP by the chicken β-actin promoter associated with the cytomegalovirus immediate-early enhancer in cochlear cells showed that each of these serotypes successfully targets distinct cochlear cell types. In contrast to the other serotypes, the AAV3 vector specifically transduced cochlear inner hair cells with high efficiency *in vivo*, while the AAV1, 2, 5, 7, and 8 vectors also transduced these and other cell types, including spiral ganglion and spiral ligament cells. There was no loss of cochlear function with respect to evoked auditory brain-stem responses over the range of frequencies tested after the injection of AAV vectors. These findings are of value for further molecular studies of cochlear inner hair cells and for gene replacement strategies to correct recessive genetic hearing loss due to monogenic mutations in these cells.

Key Words: adeno-associated virus, serotype, gene transfer, cochlea, hair cells

INTRODUCTION

The total number of hair cells in the cochlea is finite. They are not renewed and there is very little (if any) redundancy in this population. The irreversible loss of cochlear hair cells is presumed to be a fundamental cause of permanent sensorineural hearing loss. Gene transfer into hair cells presents numerous opportunities for protecting these cells. There is considerable interest in the development of viral vectors to deliver genes to the cochlea to counteract hearing impairment, and recent studies have focused on vectors based on adenovirus [1–3], herpes simplex virus [4–6], lentivirus [7], and adeno-associated virus (AAV) [8,9]. The patterns of vector-encoded transgene expression have been found to differ significantly among vectors. Cochlear hair cells can be efficiently transduced with adenovirus vectors [10–12]. However, these vectors were found to provoke a strong immune response that could damage recipient cells and compromise cochlear function [10,13,14]; they are also incapable of mediating prolonged transgene expression [15,16]. Although AAV vectors might overcome these problems, the transduction of hair cells by AAV2-derived vectors is controversial [8,10,17]. To our knowledge, other AAV serotypes have not yet been tested as cochlear gene transfer vectors *in vitro* or *in vivo*. AAV vectors are of interest in the context of gene therapy because they mediate efficient transfer and long-term stable expression of therapeutic genes in a wide variety of postmitotic tissues with minimal vector-related cytotoxicity.

In this study, we assessed the utility of seven AAV serotypes as vectors with the chicken β-actin promoter associated with a cytomegalovirus immediate-early

1525-0016/$30.00

doi:10.1016/j.ymthe.2005.03.021

enhancer (CAG)-driven enhanced green fluorescent protein (EGFP) gene [18] in the murine cochlea. Vectors were introduced by microinjection through the round window membrane [19]. As a result, we determined that the specific and efficient gene transduction of inner hair cells could be achieved by using AAV type 3 vectors.

RESULTS

Expression Profile of EGFP in the Cochlea

Several cell types line the cochlear duct and support the hair cells (Fig. 1A). We carefully made a small opening in the tympanic bulla and injected vectors derived from the AAV1–4, 7, and 8 pseudotypes into the cochlea of two strains of mice (C57BL/6J and ICR) through the round window membrane (Fig. 1B). The mode of EGFP expression in various murine cochlear hair cells had a close similarity and was essentially equal for both strains. We determined the distribution of AAV vector-mediated EGFP expression throughout the cochlea for all serotypes tested (Table 1). A principal finding is that the inner hair cells in the organ of Corti showed clear evidence of EGFP expression with all of the AAV serotype-derived vectors except for the AAV4 vector (Fig. 2). This result indicates that most of the vectors (AAV1–5, 7, and 8) could efficiently transduce cochlear inner hair cells *in vivo* when slowly infused into the scala tympani. The AAV3-based vector was the most efficient and specific of the serotypes in transducing cochlear inner hair cells (Fig. 3). Transduction with 5×10^{10} genome copies (gc)/cochlea of the AAV3 vector resulted in robust transgene expression in the inner hair cells. The spiral ganglion cells showed significantly higher levels of fluorescence per unit area with the AAV5-based vector (Fig. 2n), and the spiral ligament cells were transduced prominently with the AAV1 and AAV7 vectors (Figs. 2d and 2r). Histological sections of cochleae injected with the AAV4 vector identified EGFP-positive cells predominantly in connective tissue within the mesothelial cells beneath the organ of Corti and in mesenchymal cells lining the perilymphatic fluid spaces (Figs. 2j and 2l). Furthermore, we detected intense expression with the AAV5- and AAV8-based vectors in the inner sulcus cells and in Claudius' cells (Figs. 2p and 2x). We did not detect notable levels of gene expression in the outer hair cells, supporting pillar cells, or stria vascularis cells for any serotype.

Long-term Expression of EGFP

We examined cochlear expression of the EGFP transgene in animals sacrificed at 1–12 weeks. Expression persisted in cochlear tissues for up to 3 months after infusion, while the extent of expression peaked at 2 weeks.

Transgene Activity

We determined the percentage of inner hair cells transduced with the AAV3 vector. The mid- to high-frequency regions of the cochlea were efficiently transduced, as shown in Fig. 3. Almost all of the inner hair cells in the basal and middle cochlear regions were transduced with the AAV3 vector (Fig. 4). Transgene expression was not detected in the hair cells of the apical turn of the cochlea. The predominant expression in the middle and basal cochlear turns is reasonable, as the virus

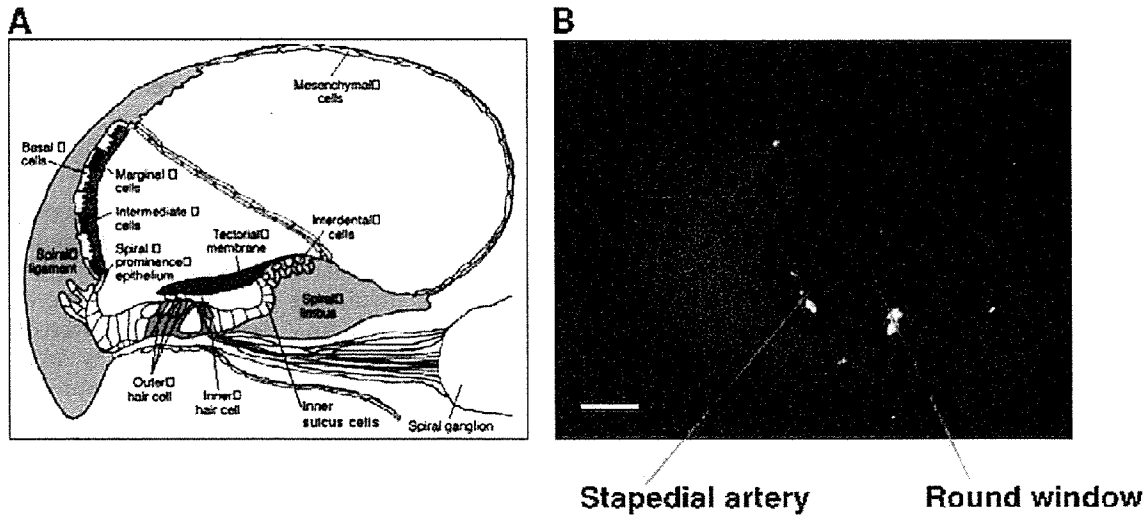

FIG. 1. (A) Schematic diagram of a cross section of the cochlea, demonstrating the scala vestibuli, scala tympani, and scala media or cochlear duct. The organ of Corti rests on the basilar membrane, with the hair cell cilia embedded in the gelatinous tectorial membrane. The outer margin of the cochlear duct contains the stria vascularis. Reproduced, by permission of the publisher, from [44]. (B) Direct visualization of the round window membrane in the right ear. The upper side of the picture is the back of the mouse and the right side is the head of the animal. The stapedial artery, a branch of the internal carotid artery, transverses an open bony semicanal within the round window niche. Bar denotes 500 μm, 15× original magnification.

TABLE 1: Expression of transgene in the mouse cochlea with vectors derived from the AAV1–4, 7, and 8 pseudotypes

Vector	Inner hair cells	Outer hair cells	Spiral ganglion	Stria vascularis	Spiral ligament	Spiral limbus	Reissner's membrane	Inner and outer pillar cells	Inner sulcus cells	Deiter's cells	Claudius' cells	Hensen's cells	Mesenchymal cells
AAV1	+++	–	++	–	++	++	++	–	+	–	–	–	++
AAV2	++	–	+	–	+	+	–	–	–	–	–	–	–
AAV3	+++	–	–	–	–	–	–	–	–	–	–	–	–
AAV4	–	–	–	–	–	–	–	–	–	–	–	–	+
AAV5	+++	–	+++	–	+	++	+	–	++	–	+	–	–
AAV7	+++	–	+	–	+++	++	–	–	+	–	+	–	++
AAV8	++++	–	–	–	+	+	–	–	++	–	+	–	+

The level of expression was graded by fluorescence intensity on a four-level scale (+, ++, +++, ++++) depending on the pixel/unit area count. ++++ means the strongest intensity of EGFP expression, + means the weakest intensity of EGFP expression, while – means no fluorescence.

was slowly infused into the scala tympani adjacent to the most basal turn of the cochlea. The percentage of transduced inner hair cells from the basal (high frequencies) to the apical (low frequencies) cochlear regions is shown in Fig. 4.

Cytotoxicity

We detected no deleterious effects on the viability of transduced cells. We compared evoked auditory brainstem response (ABR) threshold levels before and after injection, using a two-way repeated measure of the analysis of variance. There was no significant loss in ABR and hence no change in cochlear function for up to 10 days following vector infusion (Figs. 5A and 5B). In addition, the cellular and tissue architecture of experimental cochleae remained intact. There was no evidence of endolymphatic hydrops after AAV vector injection in any of the animals. We observed no significant destruction of the inner or outer hair cells (Fig. 5C).

Discussion

In the present study, we assessed the utility of vectors derived from seven AAV serotypes for gene delivery into the cochlea. Our results showed that the AAV3 vector was the most efficient and specific in transducing cochlear inner hair cells, although these cells could also be transduced with AAV1, 2, 5, 7, and 8 vectors. The transduction efficiency of the spiral ganglion by the AAV5 vector was particularly high, followed by that of the AAV1, AAV2, and AAV7 vectors. The efficient and specific transduction of inner hair cells with the AAV3 vector suggests that it recognizes a unique host range with a distinct cellular receptor. Transduction efficiency is dependent on initial viral binding (a property of the viral capsid), entry, and various postentry processes such as intracellular trafficking and second-strand synthesis [20–22]. The genome size of AAV vectors has also been demonstrated to affect transduction efficiency [23]. Comparisons of the serotypes have indicated that heterogeneity in the capsid-encoding regions and a differential ability to transduce cells may be associated with different receptor and co-receptor requirements for cell entry [24]. However, the receptors and co-receptors of AAV3 have not yet been clearly identified.

In the current study, we found that cochlear inner hair cells could be transduced with six AAV serotypes, although Lalwini *et al.* [8] reported that outer hair cells could be transduced with a low titer (1×10^6 viral particles/ml) of AAV2 *in vivo*. After injecting the AAV2 vector, we found that the spiral ganglion neurons, the inner hair cells, and the cells in the spiral ligament were all transduced. This transduction pattern differs from that reported in previous studies [8,10,17], and this discrepancy might be due to the different delivery methods and dissimilar promoters. Although the CAG promoter directs

doi:10.1016/j.ymthe.2005.03.021

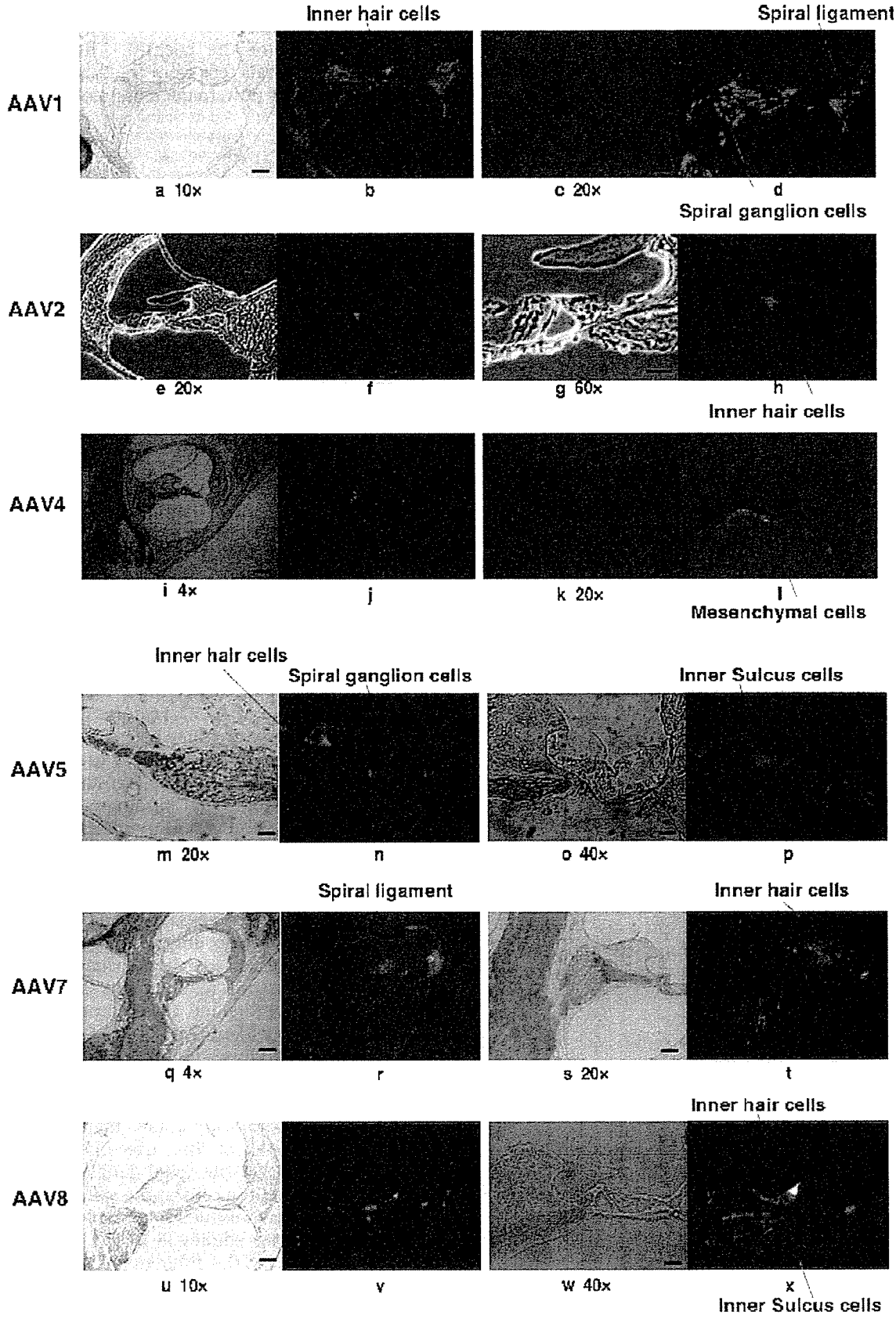

MOLECULAR THERAPY Vol. 12, No. 4, October 2005

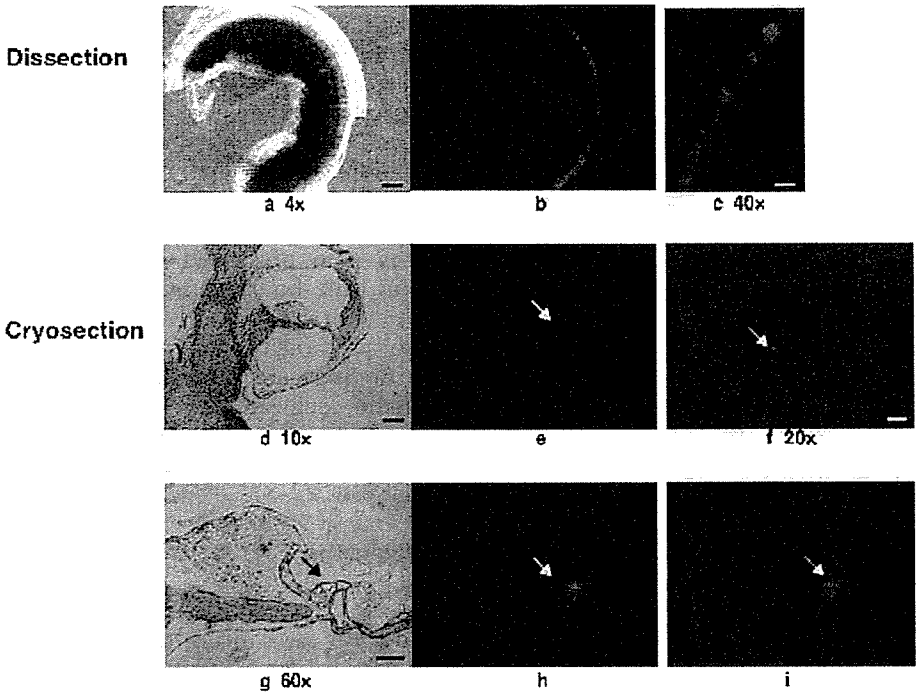

FIG. 3. Cochlear transduction with AAV3-CAG-EGFP. Dissected cochleae and cryosections show transgene expression in inner hair cells. (a) A light photomicrograph of the basal turn of the cochlea is shown, illustrating its laminar structure. (b) A fluorescence photomicrograph of this dissection. (c) A higher magnification view of the dissection shown in (b), illustrating a row of inner hair cells in the organ of Corti expressing EGFP. (d–i) Representative photomicrographs from three magnifications of a radial cochlear cryosection. (d) Light photomicrography of an intact cochlear duct. Fluorescence photomicrography of this duct is shown in (e). (h and i) A higher magnification of (e), illustrating EGFP expression within inner hair cells. Cryosections show transgene expression in the inner hair cells (arrows). Scale bars: 4×, 250 μm; 10×, 100 μm; 20×, 50 μm; 40×, 25 μm; 60×, 25 μm.

higher expression than do the cytomegalovirus (CMV) and EF-1α promoters [25], each promoter drives reporter gene expression in different cell types [26,27].

Cell-specific or -selective infectivity of the viral vectors suggests the presence of various factors to introduce the distinct expression patterns of the transgenes. Spiral ganglion neurons and glial cells can be transduced with a lentivirus–GFP construct *in vitro* but not *in vivo* [7]. The differential transducibility under *in vivo* and *in vitro* conditions reflects a high degree of structural isolation of the spiral ganglion and other cell types—such as the cells on the periphery of the endolymph—from the perilymph into which the viral vector was introduced. The strict separation of the endolymph from the perilymph is maintained by tight junctions that line the boundary between these fluid chambers. The size of the viral particle may contribute to the observed variability in transgene expression promoted by different vectors. The diameters of adenovirus and retrovirus (including lentivirus) particles are approximately 75 nm and greater than 100 nm, respectively, while the diameters of AAV vectors are typically 11–22 nm [28,29]. Thus, the larger size of lentiviruses and adenoviruses may limit their subsequent dissemination from the perilymph into the endolymph. The variable patterns of adenovirus- and lentivirus-mediated gene expression seen with different methods of inoculation may be due to the inoculation route, the volume and number of viral particles, differences in viral preparation, or differences in the method of transgene detection. The introduction of adenovirus vectors by cochleostomy or with an osmotic pump via the round window leads to a more efficient transduction of cochlear hair cells [30–32]. The apical domain (apical membrane and stereocilia) of cells in the sensory epithelium (hair cells and supporting cells) is bathed in endolymph, while the basal–lateral domain is immersed in perilymph. Access of the viral vectors to the endolymphatic space by cochleostomy may facilitate the transduction of hair cells and supporting cells. However, although the cochleostomy procedure has been tested, inoculation into the membranous labyrinth could not be confirmed [32]. In the present study, AAV vectors were found to infect cochlear hair cells easily *in vivo*, via round window injection.

Gene transfer into the cochlea through the round window membrane is ideal, because this procedure

FIG. 2. Transduction of the cochleae by AAV1-, AAV2-, AAV4-, AAV5-, AAV7-, and AAV8-based vectors. (a, c, e, g, i, k, m, o, q, s, u, and w) Light photomicrographs of cochlear cryosections. (b, d, f, h, j, l, n, p, r, t, v, and x) Fluorescence photomicrographs (green fluorescence from transgene). The spiral ligament cells were transduced prominently with the AAV1 and AAV7 vectors (d and r). Transgene expression in inner hair cells was detected with AAV1-, AAV2-, AAV5-, AAV7-, and AAV8-based vectors (b, h, n, t, and x). AAV4-based vector faintly transduced mesenchymal cells (j and l). The spiral ganglion cells showed significant levels of fluorescence with the AAV5-based vector (n). Intense fluorescence was detected with the AAV5- and AAV8-based vectors in the inner sulcus cells (p and x). Scale bars: 10×, 100 μm; 20×, 50 μm; 40×, 25 μm; 60×, 25 μm.

doi:10.1016/j.ymthe.2005.03.021

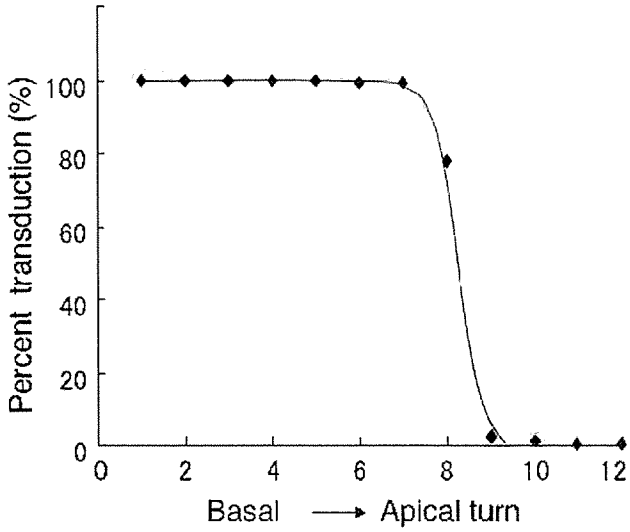

FIG. 4. EGFP expression profile of inner hair cells transduced with AAV3, as shown for a cross section subdivided into 12 segments ranging from the basal (high frequencies) to the apical (low frequencies) cochlear regions.

requires simple surgery without cochlear trauma [19]. Another critical factor in assessing the utility of a gene transfer vector is safety. Factors determining safety include the toxicity of the gene transfer agent itself, the provocation of immune responses, the generation of replication-competent virus, and the risk of creating genetically modified cells by insertional mutagenesis. The cells and tissues within the AAV-EGFP-perfused cochleae were free from inflammation and were generally intact. No pathological changes were observed in the organ of Corti, stria vascularis, or spiral ganglion cells. The long-term expression of EGFP within the cochlear tissues is consistent with data obtained from other animal models and different organ systems [9,33]. Since EGFP is known to introduce cellular toxicity, vectors expressing physiologically therapeutic proteins would achieve longer transduction periods than EGFP. Gene transfer into the inner hair cells presents numerous opportunities for auditory neuroscience. Potential applications include the localization of proteins by expression of tagged constructs, the generation of dominant-negative or antisense knockouts of endogenous proteins, the rescue of mutant phenotypes to identify disease genes, and perhaps even the treatment of auditory disorders. Advances in the molecular basis of auditory diseases have allowed the identification of a number of genetic disorders such as presbycusis, acoustic trauma, and ototoxicity. The development of gene therapy now allows us to evaluate the effects of transferring therapeutic genes into the inner ear by several different strategies. The expression of marker genes in the inner ear tissue has been demonstrated. Further studies will improve our understanding of cochlear function as well as provide for the development of novel therapies for a wide variety of inner ear diseases. Intracochlear gene transfer using AAV vectors has been established as a viable experimental proposition. Future study will include the transfer of functioning genes *in vivo* and the development of alternative vectors. While clinical application may be some way off, it is vital that gene delivery techniques are optimized in anticipation of future need.

In conclusion, the data presented in this paper demonstrate successful gene transfer into several types of cochlear cells *in vivo* with AAV-based vectors. Interestingly, the AAV3 vector promoted inner hair cell-specific transduction. These findings are of value for further molecular studies of the cochlear inner hair cells and for gene replacement strategies to correct hereditary hearing loss due to specific monogenic mutations affecting cochlear inner hair cells.

MATERIALS AND METHODS

Construction and preparation of proviral plasmids. The AAV vector proviral plasmid pAAV2-*LacZ* harbors an *Escherichia coli* β-galactosidase expression cassette with the CMV promoter, the first intron of the human growth hormone gene, and the SV40 early polyadenylation sequence, which are flanked by inverted terminal repeats (ITRs) [34]. The *LacZ* expression cassette of pAAV2-*LacZ* was ligated to *Not*I-excised pAAV5-RNL [35] to form the proviral plasmid pAAV5-*LacZ*. The pAAV2-CAG-EGFP-WPRE construct consists of the EGFP gene under the control of the CAG promoter (the chicken β-actin promoter associated with the cytomegalovirus immediate-early enhancer) and WPRE (woodchuck hepatitis virus posttranscriptional regulatory element) flanked by ITRs. The WPRE cassette augments the stability of transgene mRNA [36] and increases EGFP expression levels, thereby ensuring long-term transgene expression. A *Bam*HI–*Xba*I fragment containing the EGFP cDNA excised from pEGFP-1 and a *Hin*dIII fragment containing the WPRE sequence excised from pBS II SK$^+$WPRE-B11 (a gift from Dr. J. Donello) was ligated to *Xho*I linkers and cloned into an *Xho*I site of pCAGGS (a gift from Dr. J.-I. Miyazaki) to create pCAG-EGFP-WPRE. The EGFP expression cassette from pCAG-EGFP-WPRE was ligated to the *Not*I-excised pAAV2-*LacZ* and pAAV5-RNL [35] to form the proviral plasmids pAAV2-CAG-EGFP-WPRE and pAAV5-CAG-EGFP-WPRE, respectively. The AAV-helper plasmid harbors Rep and Cap. The adenovirus helper plasmid pAdeno5 (identical to pVAE2AE4-5) encodes the entire E2A and E4 regions and the VA RNA I and II genes [37]. Plasmids were purified with the Qiagen plasmid purification kits (Qiagen K.K., Tokyo, Japan).

Recombinant AAV vector production. Vectors derived from the AAV1–4, 7, and 8 pseudotypes were produced with the AAV packaging plasmid pAAV1RepCap (for AAV1) [38], pHLP19 (for AAV2), pAAV3RepCap (for AAV3) [39], pAAV4RepCap (for AAV4) [40], pAAV7RepCap (for AAV7) [41], or pAAV8RepCap (for AAV8) [41] and the AAV proviral plasmid pAAV2-*LacZ* or pAAV2-CAG-EGFP-WPRE. The plasmids pAAV5RepCap [35] and pAAV5-*LacZ*, or pAAV5-CAG-EGFP-WPRE, were used to produce vector with the AAV5 pseudotype [42]. Seven AAV serotype vectors were produced as previously described by the three-plasmid transfection adenovirus-free protocol [37]. Briefly, three days before transfection, 293 cells were plated onto a 10-tray Cell Factory (Nalge Nunc International, Rochester, NY, USA; 6×10^7 cells/10-tray). The cells were cotransfected with 650 μg each of the proviral plasmid, the AAV vector packaging plasmid, and the adenovirus helper plasmid pAdeno5 [34] by the calcium phosphate coprecipitation method. The medium was changed following incubation for 6–8 h at 37°C. Recombinant AAV was harvested 72 h after transfection by three freeze/thaw cycles. The crude viral lysate was purified twice on a cesium chloride two-tier centrifugation

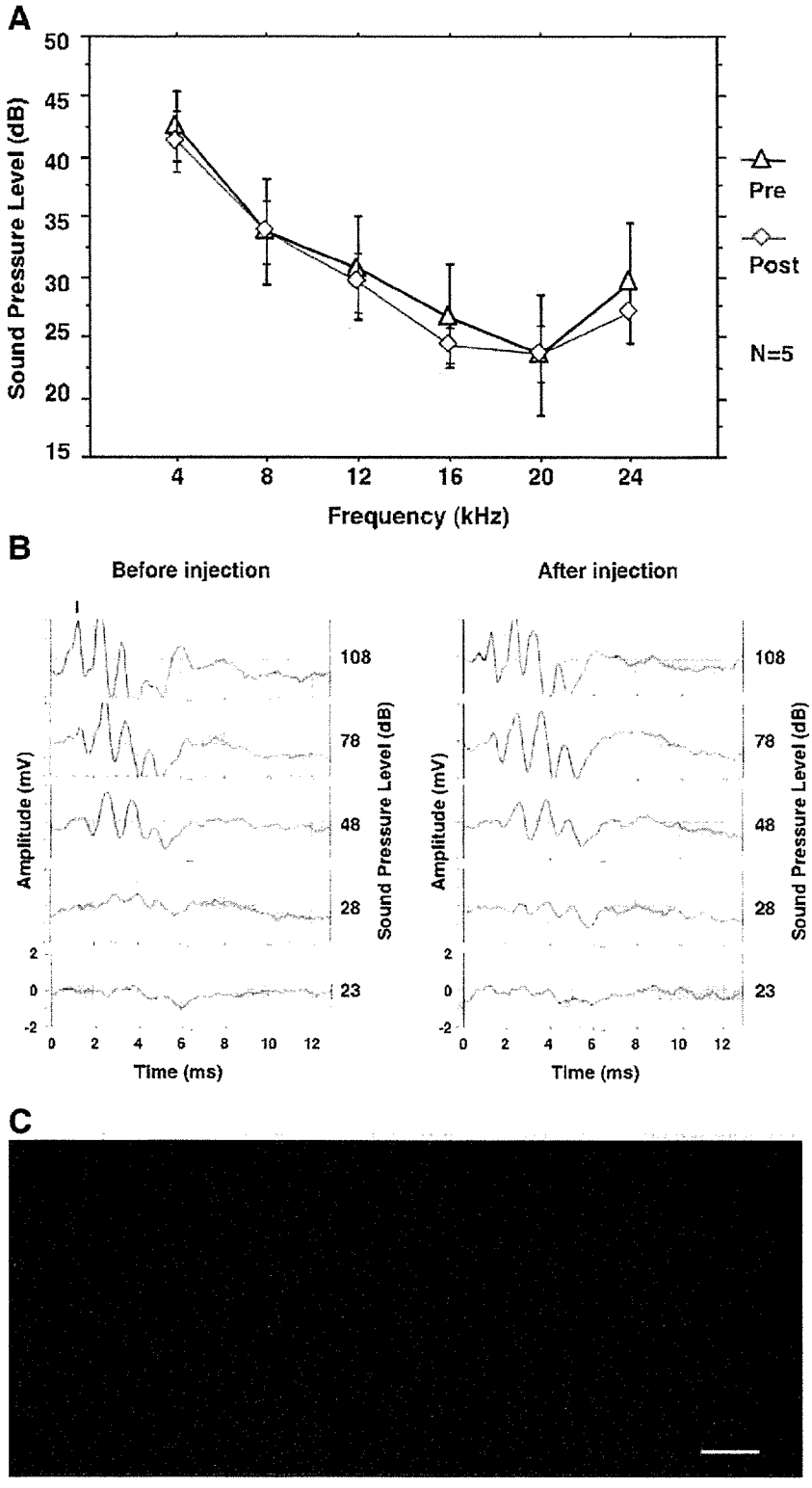

FIG. 5. (A) ABR threshold (mean ± SD) at each frequency tested preoperatively (pre) versus postoperatively (post). (B) Example of ABR waveforms in C57BL/6J at various stimuli (16 kHz; 108 dB, 78 dB, 48 dB, 28 dB, and 23 dB). ABR were tested in the transduced ear prior to viral injection and 10 days after injection. Wave I was measured to analyze the activity of the cochlea. (C) F-actin staining showing that no outer hair cells were lost from inoculated cochleae. Original magnification 40×; scale bar, 25 μm.

gradient as described previously [24]. The viral stock was treated with DNase and titrated by quantitative real-time PCR with plasmid standards [43].

Surgical procedures and cochlear perfusions. All animal studies were performed in accordance with the guidelines issued by the committee on animal research of Jichi Medical School and approved by its ethics